The current issue and full text archive of this journal is available at
www.emeraldinsight.com/0961-5539.htm

Received December 2004
Revised August 2005
Accepted October 2005

A Mach-uniform pressure-correction algorithm with AUSM+ flux definitions

Krista Nerinckx, Jan Vierendeels and Erik Dick
Department of Flow, Heat and Combustion Mechanics, Ghent University, Gent, Belgium

Abstract

Purpose – To present conversion of the advection upwind splitting method (AUSM+) from the conventional density-based and coupled formulation to the pressure-based and segregated formulation.

Design/methodology/approach – The spatial discretization is done by a finite volume method. A collocated grid cell-center formulation is used. The pressure-correction procedure is set up in the usual way for a compressible flow problem. The conventional Rhie-Chow interpolation methodology for the determination of the transporting velocity, and the conventional central interpolation for the pressure at the control volume faces, are replaced by AUSM+ definitions.

Findings – The AUSM+ flux definitions are spontaneously well suited for use in a collocated pressure-correction formulation. The formulation does not require extensions to these flux definitions. As a consequence, the results of a density-based fully coupled method, are identical to the results of a pressure-based segregated formulation. The advantage of the pressure-correction method with respect to the density-based method, is the higher efficiency for low Mach number applications. The advantage of the AUSM+ flux definition for the transporting velocity with respect to the conventional Rhie-Chow interpolation, is the improved accuracy in high Mach number flows. As a consequence, the combination of AUSM+ with a pressure-correction method leads to an algorithm with improved performance for flows at all Mach numbers.

Originality/value – A new methodology, with obvious advantages, is composed by the combination of ingredients from an existing spatial discretization method (AUSM+) and an existing time stepping method (pressure-correction).

Keywords Fluids, Finite volume methods, Fluid pressure, Flow

Paper type Research paper

1. Introduction

Originally, density-based methods, which use a coupled solution technique, were designed to handle high Mach number flows. On the other hand, segregated pressure-based algorithms like the pressure-correction method (Patankar, 1980) were developed for the incompressible and low Mach number regime. However, several applications – a cavitating flow is one example (Senocak and Shyy, 2002; Edwards *et al.*, 2000) – require algorithms that can handle a very broad Mach number range.

In order to obtain Mach-uniform algorithms, density-based methods have been extended towards the low Mach number limit by preconditioning. This means that the time derivative is changed such that the low Mach number stiffness problems is remedied. In addition, the flux definitions are adapted to scale them properly when the Mach number diminishes (Weiss and Smith, 1995; Edwards and Liou, 1998; Vierendeels *et al.*, 2001; Luo and Baum, 2003).

International Journal of Numerical Methods for Heat & Fluid Flow
Vol. 16 No. 6, 2006
pp. 718-739
© Emerald Group Publishing Limited
0961-5539
DOI 10.1108/09615530610679075

Besides that, pressure-based methods were extended to cope with high Mach numbers (Merkle *et al.*, 1992; Demirdžić *et al.*, 1993; Lien and Leschziner, 1994; Lien *et al.*, 1996; Batten *et al.*, 1996; Issa and Javareshhkian, 1998; Moukalled and Darwish, 2001; Shyy *et al.*, 1997; Bijl and Wesselling, 1998; Wenneker *et al.*, 2002; Van der Heul *et al.*, 2003). For that purpose, the pressure should act both on the velocity and the density (Moukalled and Darwish, 2001). Therefore, density too has to be corrected, resulting in a more complicated pressure-correction equation. In the incompressible and low Mach number regime, special measures have to be taken to ensure pressure-velocity coupling. A staggered grid can be used (Shyy *et al.*, 1997; Bijl and Wesselling, 1998; Wenneker *et al.*, 2002; Van der Heul *et al.*, 2003), or a collocated arrangement in combination with a special interpolation technique, called the Rhie-Chow interpolation (Rhie and Chow, 1982; Perić *et al.*, 1988). Because of its flexibility, we choose the collocated storage of variables. However, we demonstrate that the Rhie-Chow procedure gives bad results if large pressure gradients occur. It is for that reason that we propose an alternative approach, based on the advection upstream splitting method (AUSM+) (Liou and Steffen, 1993; Liou, 2000) flux definitions. Doing so, we achieve the extension of a popular numerical algorithm from a density-based to a pressure-based formulation.

2. Governing equations

A one-dimensional non-viscous flow in a tube with a variable section $S(x)$ is considered. The Euler equations governing this type of flow are the continuity, momentum and energy equation:

$$\frac{\partial \rho}{\partial t} + \frac{1}{S}\frac{\partial \rho u S}{\partial x} = 0, \tag{1}$$

$$\frac{\partial \rho u}{\partial t} + \frac{1}{S}\frac{\partial \rho u u S}{\partial x} = -\frac{\partial \rho}{\partial x}, \tag{2}$$

$$\frac{\partial \rho E}{\partial t} + \frac{1}{S}\frac{\partial \rho E u S}{\partial x} = -\frac{1}{S}\frac{\partial \rho u S}{\partial x}, \tag{3}$$

where ρ, u, p and E, respectively, represent the density, velocity, pressure and total energy. The mass flux is defined as $\dot{m} = \rho u$. The equation of state for an ideal gas completes the system of equations:

$$\rho = \frac{p}{RT}, \tag{4}$$

where R is the gas constant and T is the temperature.

The equations are nondimensionalized by choosing three reference quantities, p_r, T_r and L_r. From these, the other reference quantities are derived:

$$\rho_r = \frac{p_r}{RT_r}, \tag{5}$$

$$u_r = \sqrt{\frac{p_r}{\rho_r}}, \tag{6}$$

$$t_r = \frac{L_r}{u_r}, \tag{7}$$

$$E_r = \frac{p_r}{\rho_r}. \tag{8}$$

The extension to two-dimensional flow is straightforward. Results for a two-dimensional test case are shown in Section 6.2.

3. The discretized set of equations

3.1 Finite volume discretization

The flow domain is subdivided into a finite number of control volumes (CVs) with length Δx. The boundaries of the domain coincide with CV faces. All the variables are stored in the CV center (collocated arrangement). A finite volume method and a backward Euler time integration is used to discretize the equations. This yields:

$$\frac{\rho_i^{n+1} - \rho_i^n}{\tau} + \frac{1}{S_i}\left[(\dot{m}S)_{i+(1/2)}^{n+1} - (\dot{m}S)_{i-(1/2)}^{n+1}\right] = 0. \tag{9}$$

$$\frac{(\rho u)_i^{n+1} - (\rho u)_i^n}{\tau} + \frac{1}{S_i}\left[(\dot{m}uS)_{i+(1/2)}^{n+1} - (\dot{m}uS)_{i-(1/2)}^{n+1}\right] = -(p_{i+(1/2)} - p_{i-(1/2)})^{n+1}, \tag{10}$$

$$\begin{aligned} &\frac{(\rho E)_i^{n+1} - (\rho E)_i^n}{\tau} + \frac{1}{S_i}\left[(\dot{m}ES)_{i+(1/2)}^{n+1} - (\dot{m}ES)_{i-(1/2)}^{n+1}\right] \\ &\quad = \frac{-1}{S_i}\left((pu)_{i+(1/2)}S_{i+(1/2)} - (pu)_{i-(1/2)}S_{i-(1/2)}\right)^{n+1}, \end{aligned} \tag{11}$$

with $\tau = \Delta t/\Delta x$, and Δt the time step.

In the convective parts of (10) and (11), the transported quantity $\phi_{i+(1/2)}$ is upwinded:

$$(\dot{m}\phi)_{i+(1/2)} = \frac{1}{2}[\dot{m}_{i+(1/2)}(\phi_L + \phi_R) - |\dot{m}_{i+(1/2)}|(\phi_R - \phi_L)], \tag{12}$$

where ϕ represents u or E in the momentum or energy equation, respectively. Fist order accuracy is obtained by taking $\phi_L = \phi_i$ and $\phi_R = \phi_{i+1}$. For higher order of accuracy the L and R values are computed with the Van Leer-k approach:

$$\phi_L = \phi_i + \frac{1}{4}[(1+k)(\phi_{i+1} - \phi_i) + (1-k)(\phi_i - \phi_{i-1})], \tag{13}$$

$$\phi_R = \phi_{i+1} - \frac{1}{4}[(1+k)(\phi_{i+1} - \phi_i) + (1-k)(\phi_{i+2} - \phi_{i+1})]. \tag{14}$$

For $k = 1/3$ third order of accuracy is obtained. However, when shocks are present the minmod-limiter is used:

$$\phi_L = \phi_i + \frac{1}{2}\min\text{mod}(\phi_{i+1} - \phi_i, \phi_i - \phi_{i-1}), \tag{15}$$

$$\phi_R = \phi_{i+1} - \frac{1}{2}\min\text{mod}(\phi_{i+1} - \phi_i, \phi_{i+2} - \phi_{i+1}). \tag{16}$$

We obtain the following set of discretized equations:

$$\frac{\rho_i^{n+1} - \rho_i^n}{\tau} + \frac{1}{S_i}\left[(\dot{m}S)_{i+(1/2)}^{n+1} - (\dot{m}S)_{i-(1/2)}^{n+1}\right] = 0, \tag{17}$$

$$A_{i,i+1}^{n+1}u_{i+1}^{n+1} + A_{i,i}^{n+1}u_i^{n+1} + A_{i,i-1}^{n+1}u_{i-1}^{n+1} = -(p_{i+(1/2)} - p_{i-(1/2)})^{n+1} + \frac{(\rho u)_i^n}{\tau} + \text{HO}_i^u, \tag{18}$$

$$\begin{aligned} A_{i,i+1}^{n+1}E_{i+1}^{n+1} + A_{i,i}^{n+1}E_i^{n+1} + A_{i,i-1}^{n+1}E_{i-1}^{n+1} = {} & \frac{-1}{S_i}((puS)_{i+(1/2)} - (puS)_{i-(1/2)})^{n+1} \\ & + \frac{(\rho E)_i^n}{\tau} + \text{HO}_i^E, \end{aligned} \tag{19}$$

with:

$$A_{i,i+1}^{n+1} = \frac{S_{i+(1/2)}}{2S_i}\left(\dot{m}_{i+(1/2)}^{n+1} - \left|\dot{m}_{i+(1/2)}^{n+1}\right|\right), \tag{20}$$

$$A_{i,i}^{n+1} = \frac{S_{i+(1/2)}}{2S_i}\left(\dot{m}_{i+(1/2)}^{n+1} - \left|\dot{m}_{i+(1/2)}^{n+1}\right|\right) - \frac{S_{i-(1/2)}}{2S_i}\left(\dot{m}_{i-(1/2)}^{n+1} - \left|\dot{m}_{i-(1/2)}^{n+1}\right|\right) + \frac{\rho_i^{n+1}}{\tau}, \tag{21}$$

$$A_{i,i-1}^{n+1} = -\frac{S_{i-(1/2)}}{2S_i}\left(\dot{m}_{i-(1/2)}^{n+1} + \left|\dot{m}_{i-(1/2)}^{n+1}\right|\right), \tag{22}$$

and HO the higher order parts of the transported quantities u or E.

This set of highly coupled equations can be solved by means of a coupled solution technique. However, this involves the solution of a very large system, which is expensive. Therefore, we propose to solve this set of equations in a segregated way, namely through a pressure-correction method.

In the mass flux $\dot{m}_{i+(1/2)}$, the density is upwinded according to the sign of the transporting velocity $u_{i+(1/2)}$. The discretization of the cell face velocity $u_{i+(1/2)}$ and the cell face pressure $p_{i+(1/2)}$ yet still has to be specified. In a classical incompressible pressure-correction method, the pressure gradient is discretized centrally. For the cell face velocity a special interpolation technique is used, namely the Rhie-Chow interpolation (Rhie and Chow, 1982; Perić *et al.*, 1988). However, as we will show later, this interpolation cannot be used for a compressible flow simulation. Therefore, we replace it by AUSM+ (Liou and Steffen, 1993; Liou, 2000), which is commonly used in coupled algorithms. We will show in what way it differs from the classical Rhie-Chow interpolation, and how it leads to much better results.

Remark that an AUSM+ definition fits perfectly in the pressure-based context, due to the separate treatment of convective and acoustic parts. The latter corresponds completely with the philosophy of a pressure-based method, as was also noticed by Venkateswaran and Merkle (1997). Other flux definitions, like flux-difference splittings (Hirsch, 1990) do not apply this separate treatment, and are, therefore, less suitable to be used in a pressure-based algorithm (Issa and Javareshhkian (1998) did it anyhow).

3.2 Cell face velocity and pressure

We present now how the cell face velocity $u_{i+(1/2)}$ and pressure $p_{i+(1/2)}$ are interpolated, both in the classical approach and with the AUSM+ definitions. In Section 4 we will explain in which steps these definitions are introduced into the algorithm.

3.2.1 Classical approach: the Rhie-Chow interpolation. In an incompressible flow simulation on a collocated grid, a central discretization of the pressure gradient leads to pressure-velocity decoupling, resulting in odd-even oscillations. This problem can be remedied by a so-called Rhie-Chow interpolation for the cell face velocity $u_{i+(1/2)}$ (Rhie and Chow, 1982; Perić *et al.*, 1988). We shortly describe how it works.

From the momentum equation (18) an expression for u_i^{n+1} is derived:

$$u_i^{n+1} = \frac{-A_{i,i+1}^{n+1}u_{i+1}^{n+1} - A_{i,i-1}^{n+1}u_{i-1}^{n+1} + (\rho u)_i^n/\tau + \mathrm{HO}_i^u}{A_{i,i}^{n+1}} + \frac{-\frac{\partial p}{\partial x}\big|_i^{n+1}\Delta x}{A_{i,i}^{n+1}}. \tag{23}$$

Similarly, an expression for u_{i+1}^{n+1} is determined:

$$u_{i+1}^{n+1} = \frac{-A_{i+1,i+2}^{n+1}u_{i+2}^{n+1} - A_{i+1,i}^{n+1}u_i^{n+1} + (\rho u)_{i+1}^n/\tau + \mathrm{HO}_{i+1}^u}{A_{i+1,i+1}^{n+1}} + \frac{-\frac{\partial p}{\partial x}\big|_{i+1}^{n+1}\Delta x}{A_{i+1,i+1}^{n+1}}. \tag{24}$$

The cell face velocity $u_{i+(1/2)}^{n+1}$ is calculated as the average of these two expressions. However, both pressure gradients $\frac{\partial p}{\partial x}\big|_i$ and $\frac{\partial p}{\partial x}\big|_{i+1}$ are contracted to yield a pressure gradient over the face. This result in:

$$\begin{aligned} u_{i+(1/2)}^{n+1} = \frac{1}{2}\Bigg\{ & \frac{-A_{i,i+1}^{n+1}u_{i+1}^{n+1} - A_{i,i-1}^{n+1}u_{i-1}^{n+1} + (\rho u)_i^n/\tau + \mathrm{HO}_i^u}{A_{i,i}^{n+1}} \\ & + \frac{-A_{i+1,i+2}^{n+1}u_{i+2}^{n+1} - A_{i+1,i}^{n+1}u_i^{n+1} + (\rho u)_{i+1}^n/\tau + \mathrm{HO}_{i+1}^u}{A_{i+1,i+1}^{n+1}}\Bigg\} \\ & - \frac{1}{2}\left[\frac{1}{A_{i,i}^{n+1}} + \frac{1}{A_{i+1,i+1}^{n+1}}\right](p_{i+1}^{n+1} - p_i^{n+1}). \end{aligned} \tag{25}$$

The important feature of this expression is that the cell face velocity depends on the pressure values at the two neighbor nodes, which is also the basis of the staggering principle (Perić *et al.*, 1988). With:

$$\frac{1}{A_{i+(1/2)}^{n+1}} \equiv \frac{1}{2}\left[\frac{1}{A_{i,i}^{n+1}} + \frac{1}{A_{i+1,i+1}^{n+1}}\right], \tag{26}$$

Equation (25) can also be written as:

$$u_{i+(1/2)}^{n+1} = \underbrace{\frac{1}{2}(u_i^{n+1} + u_{i+1}^{n+1})}_{\textit{linear interpolation}} + \underbrace{\frac{1}{2}\left[\frac{p_{i+1}^{n+1} - p_{i-1}^{n+1}}{2A_{i,i}^{n+1}} + \frac{p_{i+2}^{n+1} - p_i^{n+1}}{2A_{i+1,i+1}^{n+1}}\right] - \left(\frac{p_{i+1}^{n+1} - p_i^{n+1}}{A_{i+(1/2)}^{n+1}}\right)}_{\textit{pressure smoothing}}. \tag{27}$$

Thus, the Rhie-Chow interpolation introduces a pressure smoothing term into the momentum equations. It is instructive to note that, with the assumption $A_{i,i} = A_{i+1,i+1} = A_{i+(1/2)}$, the pressure smoothing term that is added to the linear interpolation turns out to be:

$$\frac{1}{4A}(p_{i+2} - 3p_{i+1} + 3p_i - p_{i-1}), \tag{28}$$

which is in essence a third-order dissipation term. Since the face velocity $u^{n+1}_{i+(1/2)}$ enters the convective flux of the momentum equation, the Rhie-Chow interpolation introduces a fourth-order smoothing term into the momentum equation, even if $\partial p/\partial x$ is approximated by central differencing (Lien *et al.*, 1996; Davidson, 1996).

Thus, in the classical approach, $u^{n+1}_{i+(1/2)}$ is discretized with the interpolation formula (27). $p^{n+1}_{i+(1/2)}$ is discretized centrally:

$$p^{n+1}_{i+(1/2)} = \frac{\left(p^{n+1}_i + p^{n+1}_{i+1}\right)}{2}.$$

Also $(pu)^{n+1}_{i+(1/2)}$ in the RHS of the energy equation is discretized centrally:

$$(pu)^{n+1}_{i+(1/2)} = \frac{\left((pu)^{n+1}_i + (pu)^{n+1}_{i+1}\right)}{2}.$$

3.2.2 AUSM+. In the advection upwind splitting method (AUSM+), the cell face velocity $u_{i+(1/2)}$ is determined by a Mach-dependent interpolation:

$$u^{n+1}_{i+(1/2)} = a^{n+1}_{1/2} m^{n+1}_{1/2}, \tag{29}$$

$$m^{n+1}_{1/2} = M^{+}_{(4)}\left(M^{n+1}_L\right) + M^{-}_{(4)}\left(M^{n+1}_R\right), \tag{30}$$

with an appropriate definition for the common speed of sound $a_{(1/2)}$ (Liou, 1996), and:

$$M^{n+1}_{L/R} = \frac{u^{n+1}_{L/R}}{a^{n+1}_{1/2}}, \tag{31}$$

$$M^{\pm}_{(4)} = \begin{cases} \pm\frac{1}{4}(M \pm 1)^2 \pm \frac{1}{8}(M^2 - 1)^2, & |M| < 1 \\ M^{\pm}_{(1)}, & \text{otherwise} \end{cases} \tag{32}$$

$$M^{\pm}_{(1)} = \frac{1}{2}(M \pm |M|). \tag{33}$$

Also for the cell face pressure $p_{i+(1/2)}$ a Mach-dependent interpolation is defined:

$$p^{n+1}_{i+(1/2)} = P^{+}_{(5)}\left(M^{n+1}_L\right)p^{n+1}_L + P^{-}_{(5)}\left(M^{n+1}_R\right)p^{n+1}_R, \tag{34}$$

$$P_{(5)}^{\pm} = \begin{cases} \frac{1}{4}(M \pm 1)^2(2 \mp M) \pm \frac{3}{16}M(M^2-1)^2, & |M| < 1 \\ \frac{1}{2M}(M \pm |M|), & \text{otherwise} \end{cases} \tag{35}$$

In the RHS of the energy equation (19), the pressure is upwinded, so that $\rho H = \rho E + p$ is upwinded:

$$(pu)_{i+(1/2)}^{n+1} = \frac{1}{2}\left[u_{i+(1/2)}^{n+1}\left(p_L^{n+1} + p_R^{n+1}\right) - \left|u_{i+(1/2)}^{n+1}\right|\left(p_R^{n+1} - p_L^{n+1}\right)\right], \tag{36}$$

and $u_{i+(1/2)}$ is calculated with the AUSM+ definition (29). The L and R values are determined with (13 and 14) or (15 and 16).

For low Mach number flow, special measures have to be taken with regard to the scaling of the flux and to ensure pressure-velocity coupling.

3.2.2.1 Scaling. The diffusive contributions in the AUSM+ fluxes scale badly when the Mach number diminishes (Edwards and Liou, 1998). Edwards and Liou remedy this problem by introducing preconditioned Mach numbers and a preconditioned speed of sound:

$$\tilde{M}_{L/R} = \frac{1}{f_{1/2}}M_{L/R} = \frac{u_{L/R}}{\tilde{a}_{1/2}}, \tag{37}$$

$$\tilde{a}_{1/2} \equiv f_{1/2}a_{1/2}, \tag{38}$$

with:

$$f_{1/2} = \frac{\sqrt{\left(1 - M_{\mathrm{ref}(1/2)}^2\right)^2 M_{1/2}^2 + 4M_{\mathrm{ref}(1/2)}^2}}{\left(1 + M_{\mathrm{ref}(1/2)}^2\right)}. \tag{39}$$

M_{ref} equals the local Mach number in subsonic flow. In supersonic regions it is given the constant value 1. The 1/2 notation indicates the evaluation using simple arithmetic averages. The new definitions of the left- and right-state Mach numbers:

$$\bar{M}_L = \frac{1}{2}\left[\left(1 + M_{\mathrm{ref}(1/2)}^2\right)\tilde{M}_L + \left(1 - M_{\mathrm{ref}(1/2)}^2\right)\tilde{M}_R\right], \tag{40}$$

$$\bar{M}_R = \frac{1}{2}\left[\left(1 + M_{\mathrm{ref}(1/2)}^2\right)\tilde{M}_R + \left(1 - M_{\mathrm{ref}(1/2)}^2\right)\tilde{M}_L\right], \tag{41}$$

and the new definition for $\tilde{a}_{1/2}$ (equation (38)) replace the conventional definitions in both the convective and pressure components of the interface flux.

This scaling problem is purely a problem of the flux definition, it has nothing to do with the solution technique. Thus, it also occurs when we apply AUSM+ in the pressure-correction method. Therefore, we use the AUSM+ in its preconditioned version.

3.2.2.2 Pressure-velocity coupling. A second problem is the lack of pressure-velocity coupling in the low Mach number regime. From (32) and (35) it can be seen that for low Mach numbers, the AUSM+ definitions behave like central discretizations, resulting in

odd-even oscillations. In fact, it was just to prevent the latter, that the pressure smoothing term was introduced by the Rhie-Chow interpolation. Edwards and Liou (1998) introduce the pressure-velocity coupling by adding a pressure diffusion component to the AUSM+ definition of the mass flux:

$$\begin{aligned}\dot{m}_{i+(1/2)} = \dot{m}_{i+(1/2)\mathrm{AUSM+}} &+ \tilde{a}_{1/2}\left(\frac{1}{M^2_{\mathrm{ref}(1/2)}} - 1\right) \\ &\times \left[M^+_{(4)}(\bar{M}_L) - M^+_{(1)}(\bar{M}_L) - M^-_{(4)}(\bar{M}_R) + M^-_{(1)}(\bar{M}_R)\right] \\ &\times \frac{(p_L - p_R)}{(p_L/\rho_L) + (p_R/\rho_R)}.\end{aligned} \tag{42}$$

Notice that in sonic and supersonic regions M_{ref} equals one, so that the pressure diffusion term vanishes.

4. Pressure-correction algorithm

The solution of the set (17)-(19) is obtained in a segregated manner, through the SIMPLE approach (Patankar and Spalding, 1972). The known, old time level is denoted as n. The unknown, new time level is $n + 1$. To determine the state at the new time level $n + 1$, several iteration steps are taken within one time step. In a certain iteration step, we consider an iteration level k and $k + 1$. The state at level k is known from the previous iteration step. In the first iteration step, it is initialized by the level n values. The state at level $k + 1$ is to be determined. After a certain number of iteration steps, a good approximation for the state at $n + 1$ is obtained. Every single iteration steps consists of a predictor and a corrector step. The different levels in the procedure are summarized underneath:

$$\begin{array}{l}\vdots \\ \text{time level } n \\ \text{time level } n+1 \left\{ \begin{array}{l} \vdots \\ \text{iteration step } k \\ \text{iteration step } k+1 \left\{ \begin{array}{l} \text{predictor} \\ \text{corrector} \end{array} \right. \\ \vdots \end{array} \right. \\ \vdots \end{array}$$

4.1 Predictor step

First, a predictor step is taken by means of the momentum equation (18) and the energy equation (19). The mass fluxes $\dot{m}_{i+(1/2)}$ and density ρ_i in the coefficients A are put at the known iteration level k. Also the pressure, the (pu)-terms and the HO-terms in the RHS are written at level k. Predictor values u_i^* and E_i^* are obtained from:

$$A^k_{i,i+1}u^*_{i+1} + A^k_{i,i}u^*_i + A^k_{i,i-1}u^*_{i-1} = -\left(p^k_{i+(1/2)} - p^k_{i-(1/2)}\right) + \frac{(\rho u)^n_i}{\tau} + \mathrm{HO}^{u,k}_i, \quad (43)$$

$$A^k_{i,i+1}E^*_{i+1} + A^k_{i,i}E^*_i + A^k_{i,i-1}E^*_{i-1} = \frac{-1}{S_i}\left((puS)^k_{i+(1/2)} - (puS)^k_{i-(1/2)}\right) + \frac{(\rho E)^n_i}{\tau} + \mathrm{HO}^{E,k}_i. \quad (44)$$

The mass fluxes $\dot{m}^k_{i+(1/2)}$ are known from the previous iteration step. They are not interpolated at this point of the procedure. The way to calculate $p^k_{i+(1/2)}$ and $(pu)^k_{i+(1/2)}$ depends on the considered approach. In the classical approach, they are calculated as:

$$p^k_{i+(1/2)} = \frac{\left(p^k_i + p^k_{i+1}\right)}{2} \quad \text{and} \quad (pu)^k_{i+(1/2)} = \frac{\left((pu)^k_i + (pu)^K_{i+1}\right)}{2}.$$

In the AUSM approach they are Mach-dependently interpolated from level k values with (29) and (34).

From the predictor values u^*_i and E^*_i, a predictor value for the temperature is determined:

$$T^*_i = \frac{\gamma - 1}{R}\left(E^*_i - \frac{1}{2}\left(u^*_i\right)^2\right), \quad (45)$$

where γ is the specific heat ratio.

Thus, after the predictor step, an intermediate state (p^k, u^*, T^*) is obtained. The temperature is updated by this value, i.e.:

$$T^{k+1}_i = T^*_i. \quad (46)$$

4.2 Corrector step

As in the incompressible pressure-correction method, the continuity equation is considered as a constraint instead of being advanced in time:

$$\frac{\rho^{k+1}_i - \rho^n_i}{\tau} + \frac{1}{S_i}\left[(\dot{m}S)^{k+1}_{i+(1/2)} - (\dot{m}S)^{k+1}_{i-(1/2)}\right] = 0. \quad (47)$$

Corrections with regard to the intermediate state * are defined:

$$p' = p^{k+1} - p^k, \quad (48)$$

$$u' = u^{k+1} - u^*. \quad (49)$$

In the compressible case, the density too has to be corrected:

$$\rho' = \rho^{k+1} - \rho^*, \quad (50)$$

with:

$$\rho^* = \frac{p^k}{RT^*}. \tag{51}$$

This will result in a more complicated pressure-correction equation than in the incompressible case; the character is altered from pure diffusive to mixed convective-diffusive (Senocak and Shyy, 2002). To derive this pressure-correction equation, the mass flux in the continuity equation (47) is expanded as:

$$\dot{m}^{k+1}_{i+(1/2)} = \dot{m}^*_{i+(1/2)} + \rho'_{i+(1/2)} u^*_{i+(1/2)} + \rho^*_{i+(1/2)} u'_{i+(1/2)}. \tag{52}$$

Since the density is the transported quantity in the continuity equation, it is upwinded:

$$\dot{m}^*_{i+(1/2)} = \frac{1}{2}\left[u^*_{i+(1/2)}\left(\rho^*_L + \rho^*_R\right) - \left|u^*_{i+(1/2)}\right|\left(\rho^*_R - \rho^*_L\right)\right]. \tag{53}$$

In the last term of equation (52), $\rho^*_{i+(1/2)}$ is also upwinded according to the sign of $u^*_{i+(1/2)}$. Notice that the latter does not affect the accuracy of the final solution, since corrections become zero when convergence is reached (Issa and Javareshhkian, 1998). The way to calculate $u^*_{i+(1/2)}$ depends on the considered approach. In the classical approach, the Rhie-Chow interpolation formula (27) is used, with values at the intermediate state (u^*, p^k). In the AUSM approach, we use (29).

4.2.1 Density correction. The density corrections are upwinded:

$$\rho'_{i+(1/2)} u^*_{i+(1/2)} = \frac{1}{2}\left[u^*_{i+(1/2)}(\rho'_i + \rho'_{i+1}) - \left|u^*_{i+(1/2)}\right|(\rho'_{i+1} + \rho'_i)\right], \tag{54}$$

where only the first order part is corrected. They are related to the pressure corrections by:

$$\rho' = \left.\frac{\partial \rho}{\partial p}\right|^*_{T=\text{cte}} \cdot p' \equiv C^*_\rho p'. \tag{55}$$

The coefficient C_ρ is determined from the equation of state (4):

$$C^*_\rho = \frac{1}{RT^*}. \tag{56}$$

Again, the value of C_ρ will not affect the final solution because of its multiplication with a correction.

4.2.2 Velocity correction. A relation between the velocity corrections $u'_{i+(1/2)}$ and pressure corrections p'_i follows from the momentum equation. We write equation (18) as:

$$A^k_{i,i+1} u^*_{i+1} + A^k_{i,i} u^{k+1}_i + A^k_{i,i-1} u^*_{i-1} = -\left.\frac{\partial \rho}{\partial x}\right|^{k+1}_i \Delta x + \frac{(\rho u)^n_i}{\tau} + \text{HO}^{u,k}_i. \tag{57}$$

By subtracting the predictor equation (43), we obtain:

$$u'_i = -\frac{1}{A^k_{i,i}} \left.\frac{\partial p'}{\partial x}\right|_i \Delta x. \tag{58}$$

A similar expression can be derived for u'_{i+1}. Taking the average of these two expressions, and contracting the pressure gradients, gives:

$$u'_{i+(1/2)} = -\frac{1}{A^k_{i+(1/2)}}(p'_{i+1} - p'_i). \tag{59}$$

4.2.3 Pressure correction. By substitution of the former into the discretized continuity equation (47), the following pressure-correction equation is obtained:

$$B^*_{i,i+1}p'_{i+1} + B^*_{i,i}p'_i + B^*_{i,i-1}p'_{i-1} = -\left[\frac{\rho^k_i + \rho^n_i}{\tau} + \frac{S_{i+(1/2)}}{S_i}\dot{m}^*_{i+(1/2)} - \frac{S_{i-(1/2)}}{S_i}\dot{m}^*_{i-(1/2)}\right], \tag{60}$$

with:

$$B^*_{i,i+1} = \frac{S_{i+(1/2)}}{S_i}\left[C^*_{\rho,i+1}\frac{1}{2}\left(u^*_{i+(1/2)} - \left|u^*_{i+(1/2)}\right|\right) - \frac{\rho^*_{i+(1/2)}}{A^k_{i+(1/2)}}\right], \tag{61}$$

$$\begin{aligned} B^*_{i,i} = {} & \frac{C^*_{\rho,i}}{\tau} + \frac{S_{i+(1/2)}}{S_i}\left[C^*_{\rho,i}\frac{1}{2}\left(u^*_{i+(1/2)} + \left|u^*_{i+(1/2)}\right|\right) + \frac{\rho^*_{i+(1/2)}}{A^k_{i+(1/2)}}\right] \\ & - \frac{S_{i-(1/2)}}{S_i}\left[C^*_{\rho,i}\frac{1}{2}\left(u^*_{i-(1/2)} - \left|u^*_{i-(1/2)}\right|\right) + \frac{\rho^*_{i-(1/2)}}{A^k_{i-(1/2)}}\right], \end{aligned} \tag{62}$$

$$B^*_{i,i-1} = \frac{S_{i-(1/2)}}{S_i}\left[C^*_{\rho,i-1}\frac{1}{2}\left(u^*_{i-(1/2)} + \left|u^*_{i-(1/2)}\right|\right) + \frac{\rho^*_{i-(1/2)}}{A^k_{i-(1/2)}}\right]. \tag{63}$$

This set of equations is solved for the pressure corrections p'_i.

4.3 Updates

The pressure is updated as:

$$p^{k+1}_i = p^k_i + p'_i \tag{64}$$

Equation (55) gives the density corrections ρ'_i The density is updated as:

$$\rho^{k+1}_i = \rho^*_i + \rho'_i \tag{65}$$

Equations (54) and (59) give the density corrections $\rho'_{i+(1/2)}$ and the velocity corrections $u'_{i+(1/2)}$, respectively. From equation (52) the mass flux $\dot{m}^{k+1}_{i+(1/2)}$ is updated. Its value is used in the next iteration step.

Velocity corrections are calculated with (58). In the classical approach, the pressure gradient is discretized centrally. In the AUSM approach, the pressure gradient is written as:

$$\left.\frac{\partial p'}{\partial x}\right|_i \Delta x = p'_{i+(1/2)} - p'_{i-(1/2)}, \tag{66}$$

and the face values are Mach-dependently interpolated with (34). The velocity is updated as:

$$u_i^{k+1} = u_i^* + u'_i. \tag{67}$$

To summarize, we run through the different steps of the algorithm:

- All node values are assumed to be known at the old time level n, and at the previous iteration level k. Also the mass flux $\dot{m}^k_{i+(1/2)}$ was calculated in the previous iteration step.
- The coefficients A^k are calculated with (20)-(22). The RHS of equations (43) and (44) are calculated. In the classical approach $p^k_{i+(1/2)}$ and $(\mathrm{pu})^k_{i+(1/2)}$ are interpolated centrally from level k values. In the AUSM approach they are calculated with (34) and (36).
- Predictor values u_i^* and E_i^* are determined from (43) and (44), respectively. T_i^* is calculated with (45), ρ_i^* with (51). T_i is updated, (46).
- $u^*_{i+(1/2)}$ is calculated. In the classical approach, The Rhie-Chow interpolation (27) is used. In the AUSM approach, we use (29). $\rho^*_{i+(1/2)}$ is calculated (upwind). $\dot{m}^*_{i+(1/2)}$ is calculated with (53). The coefficients B^* are calculated with (61)-(63).
- The pressure-correction equation (60) is solved. The pressure is updated, (64).
- Density corrections are determined with (55). The density is updated, (65).
- The mass flux $\dot{m}^k_{i+(1/2)}$ is updated with (52), (54) and (59).
- Velocity corrections are calculated with (58). The velocity is updated, (67).
- A next iteration step is started unless convergence was reached.

5. Boundary conditions

The boundaries of the computational domain coincide with the cell faces $1 - 1/2$ (inlet) and $\mathrm{N} + 1/2$ (outlet). The boundary conditions (BCs) are introduced in a way similar to those presented by Demirdžić *et al.* (1993). For brevity, we consider only subsonic in and outlet conditions.

5.1 Inlet conditions

Since the inlet is assumed to be subsonic, one numerical and two physical BCs have to be imposed. As a numerical BC, a first order extrapolation of the Mach number is performed; as physical BCs the total pressure $p_{0,\mathrm{in}}$ and the total temperature $T_{0,\mathrm{in}}$ are prescribed.

Thus:

$$M_{1-(1/2)} = M_1, \tag{68}$$

$$p_{0,1-(1/2)} = p_{0,\mathrm{in}}, \tag{69}$$

$$T_{0,1-(1/2)} = T_{0,\mathrm{in}}. \tag{70}$$

5.1.1 Finite volume method. The equations (9)-(11) are written for $i = 1$. Since no upwinding can be applied at the face $1 - (1/2)$, we get the following set of discretized equations:

$$\frac{\rho_1^{n+1} - \rho_1^n}{\tau} + \frac{1}{S_1}\left[(\dot{m}S)_{1+(1/2)}^{n+1} - (\dot{m}S)_{1-(1/2)}^{n+1}\right] = 0, \tag{71}$$

$$\begin{aligned} A_{1,2}^{n+1}u_2^{n+1} + A_{1,1}^{n+1}u_1^{n+1} &= (p_{1+(1/2)} - p_{1-(1/2)})^{n+1} \\ &\quad + \frac{S_{1-(1/2)}}{S_1}\dot{m}_{1-(1/2)}^{n+1}u_{1-(1/2)}^{n+1} + \frac{(\rho u)_1^n}{\tau} + \mathrm{HO}_1^u, \end{aligned} \tag{72}$$

$$\begin{aligned} A_{1,2}^{n+1}E_2^{n+1} + A_{1,1}^{n+1}E_1^{n+1} &= \frac{-1}{S_1}\left((puS)_{1+(1/2)}^{n+1} - (puS)_{1-(1/2)}^{n+1}\right) \\ &\quad + \frac{S_{1-(1/2)}}{S_1}\dot{m}_{1-(1/2)}^{n+1}E_{1-(1/2)}^{n+1} + \frac{(\rho E)_1^n}{\tau} + \mathrm{HO}_1^E, \end{aligned} \tag{73}$$

with:

$$A_{1,2}^{n+1} = \left[A_{i,i+1}^{n+1}\right]_{i=1}, \tag{74}$$

$$A_{1,1}^{n+1} = \frac{S_{1+(1/2)}}{2S_1}\left(\dot{m}_{1+(1/2)}^{n+1} + \left|\dot{m}_{1+(1/2)}^{n+1}\right|\right) + \frac{\rho_1^{n+1}}{\tau}. \tag{75}$$

5.1.2 Inlet face variables. An expression for the transported quantities $u_{1-(1/2)}^{n+1}$ and $E_{1-(1/2)}^{n+1}$ is derived from the BCs (68) and (70):

$$T_{1-(1/2)}^{n+1} = \frac{T_{0,\mathrm{in}}}{1 + ((\gamma - 1)/2)\left(M_1^{n+1}\right)^2}, \tag{76}$$

$$u_{1-(1/2)}^{n+1} = M_1^{n+1}\sqrt{\gamma R T_{1-(1/2)}^{n+1}}, \tag{77}$$

$$E_{1-(1/2)}^{n+1} = \frac{R}{\gamma - 1}T_{1-(1/2)}^{n+1} + \frac{1}{2}\left(u_{1-(1/2)}^{n+1}\right)^2. \tag{78}$$

An expression for $p_{1-(1/2)}^{n+1}$ is derived from the BCs (68) and (69):

$$p_{1-(1/2)}^{n+1} = \frac{p_{0,\mathrm{in}}}{\left(1 + ((\gamma - 1)/2)\left(M_1^{n+1}\right)^2\right)^{(\gamma/(\gamma-1))}}. \tag{79}$$

In the mass flux $\dot{m}_{1-(1/2)}^{n+1}$, the density $\rho_{1-(1/2)}^{n+1}$ is calculated as:

$$\rho_{1-(1/2)}^{n+1} = \frac{p_{0,\mathrm{in}}}{RT_{0,\mathrm{in}}}\frac{1}{\left(1 + ((\gamma - 1)/2)\left(M_1^{n+1}\right)^2\right)^{1/\gamma - 1}}. \tag{80}$$

The transporting, velocity $u_{1-(1/2)}^{n+1}$ is calculated with (77). Remark that at the face $1 + (1/2)$, The Rhie-Chow interpolation formula differs slightly from (27):

$$u_{1+(1/2)}^{n+1} = \frac{1}{2}\left(u_1^{n+1} + u_2^{n+1}\right) + \frac{1}{2}\left[\frac{1}{A_{1,1}^{n+1}}\left(\frac{p_1^{n+1} + p_2^{n+1}}{2} - p_{1-(1/2)}^{n+1}\right) + \frac{p_3^{n+1} - p_1^{n+1}}{2A_{2,2}^{n+1}}\right] - \left(\frac{p_2^{n+1} - p_1^{n+1}}{A_{1+(1/2)}^{n+1}}\right). \tag{81}$$

5.1.3 Predictor step. The predictor equations for that first node read:

$$A_{1,2}^k u_2^* + A_{1,1}^k u_1^* = -\left(p_{1+(1/2)}^k - p_{1-(1/2)}^k\right) + \frac{(\rho u)_1^n}{\tau} + \mathrm{HO}_1^{u,k} + \frac{S_{1-(1/2)}}{S_1}\dot{m}_{1-(1/2)}^k u_{1-(1/2)}^k, \tag{82}$$

$$A_{1,2}^K E_2^* + A_{1,1}^K E_1^* = \frac{-1}{S_1}\left((puS)_{1+(1/2)}^k - (puS)_{1-(1/2)}^k\right) + \frac{(\rho E)_1^n}{\tau} + \mathrm{HO}_1^{E,k} + \frac{S_{1-(1/2)}}{S_1}\dot{m}_{1-(1/2)}^k E_{1-(1/2)}^k, \tag{83}$$

where $u_{1-(1/2)}^k$, $p_{1-(1/2)}^k$ and $E_{1-(1/2)}^k$ are calculated with (77), (79) and (78), respectively. As for internal nodes, the mass flux $\dot{m}_{1-(1/2)}^k$ is assumed to be known from the previous iteration.

5.1.4 Corrector step. In the continuity equation for the first cell:

$$\frac{\rho_1^{k+1} - \rho_1^n}{\tau} + \frac{1}{S_1}\left[(\dot{m}S)_{1+(1/2)}^{k+1} - (\dot{m}S)_{1-(1/2)}^{k+1}\right] = 0, \tag{84}$$

only the velocity is corrected at the inlet face (Demirdžić *et al.*, 1993):

$$\dot{m}_{1-(1/2)}^{k+1} = \rho_{1-(1/2)}^*\left(u_{1-(1/2)}^* + u'_{1-(1/2)}\right). \tag{85}$$

$\rho_{1-(1/2)}^*$ is calculated with (80). The velocity correction $u'_{1-(1/2)}$ is related to the pressure corrections as:

$$u'_{1-(1/2)} = \left(\frac{\partial u}{\partial p}\right)_{1-(1/2)}^* \cdot p'_{1-(1/2)} = \left(\frac{\partial u}{\partial p}\right)_{1-(1/2)}^* \cdot \frac{1}{2}(3p'_1 - p'_2), \tag{86}$$

where a linear extrapolation (for a structured grid) was applied for the pressure correction. The coefficient is written as:

$$\left(\frac{\partial u}{\partial p}\right)_{1-(1/2)}^* = \left(\frac{\partial u_{1-(1/2)}}{\partial M1}\right)^* \left(\frac{\partial M_1}{\partial p_{1-(1/2)}}\right)^*, \tag{87}$$

and the two derivatives are calculated using the BCs (77), (76) and (79), respectively. We get:

$$\left(\frac{\partial u_{1-(1/2)}}{\partial M_1}\right) = \sqrt{\frac{\gamma \mathrm{T}_{0,\mathrm{in}}}{\arg}} - M_1^2 \sqrt{\frac{\arg}{\gamma \mathrm{T}_{0,\mathrm{in}}}} \frac{(\gamma-1)\gamma T_{0,\mathrm{in}}}{2(\arg)^2}, \tag{88}$$

$$\arg = 1 + \frac{(\gamma-1)}{2} M_1^2, \tag{89}$$

$$\frac{\partial M_1}{\partial p_{1-(1/2)}} = -\frac{1}{\gamma}\left\{\frac{2}{\gamma-1}\left[\left(\frac{p_{0,\mathrm{in}}}{p_{1-(1/2)}}\right)^{(\gamma-1)/\gamma} - 1\right]\right\}^{1/2} \frac{\left(p_{0,\mathrm{in}}\right)^{(\gamma-1)/\gamma}}{\left(p_{1-(1/2)}\right)^{(2\gamma-1)/\gamma}}. \tag{90}$$

By introducing all this into the continuity equation (84), the following pressure-correction equation is obtained:

$$B^*_{1,2} p'_2 + B^*_{1,1} p'_1 = -\left[\frac{\rho_1^k - \rho_1^n}{\tau} + \frac{S_{1+(1/2)}}{S_1} \dot{m}^*_{1+(1/2)} - \frac{S_{1-(1/2)}}{S_1} \dot{m}^*_{1-(1/2)}\right], \tag{91}$$

with:

$$\begin{aligned} B^*_{1,2} = {} & \frac{S_{1+(1/2)}}{S_1}\left[C^*_{\rho,2}\frac{1}{2}\left(u^*_{1+(1/2)} - \left|u^*_{1+(1/2)}\right|\right) - \frac{\rho^*_{1+(1/2)}}{A^k_{1+(1/2)}}\right] \\ & + \frac{S_{1-(1/2)}}{S_1}\left[\frac{1}{2}\rho^*_{1-(1/2)}\left(\frac{\partial u}{\partial p}\right)^*_{1-(1/2)}\right], \end{aligned} \tag{92}$$

$$\begin{aligned} B^*_{1,1} = {} & \frac{C^*_{\rho,1}}{\tau} + \frac{S_{1+(1/2)}}{S_1}\left[C^*_{\rho,1}\frac{1}{2}\left(u^*_{1+(1/2)} + \left|u^*_{1+(1/2)}\right|\right) + \frac{\rho^*_{1+(1/2)}}{A^k_{1+(1/2)}}\right] \\ & - \frac{S_{1-(1/2)}}{S_1}\left[\frac{3}{2}\rho^*_{1-(1/2)}\left(\frac{\partial u}{\partial p}\right)^*_{1-(1/2)}\right]. \end{aligned} \tag{93}$$

5.2 Outlet conditions

As a single physical BC at the outlet face $N + (1/2)$, the pressure is prescribed:

$$p_{N+(1/2)} = p_{\mathrm{out}}. \tag{94}$$

As numerical BCs, the total pressure and the total temperature are extrapolated:

$$p_{0,N+(1/2)} = p_{0,N} = p_N\left(1 + \frac{\gamma-1}{2} M_N^2\right)^{(\gamma/(\gamma-1))}, \tag{95}$$

$$T_{0,N+(1/2)} = T_{0,N} = T_N\left(1 + \frac{\gamma-1}{2} M_N^2\right). \tag{96}$$

From this, all needed variables can be derived:

$$M_{N+(1/2)} = \sqrt{\frac{2}{\gamma-1}\left[\left(\frac{p_{0,N+(1/2)}}{p_{N+(1/2)}}\right)^{(\gamma-1)/\gamma} - 1\right]}, \tag{97}$$

$$T_{N+(1/2)} = \frac{T_{0,N+(1/2)}}{1 + ((\gamma-1)/2))\left(M_{N+(1/2)}\right)^2}, \tag{98}$$

$$u_{N+(1/2)} = M^{n+1}_{N+(1/2)}\sqrt{\gamma R T_{N+(1/2)}}, \tag{99}$$

$$E_{N+(1/2)} = \frac{R}{\gamma-1}T_{N+(1/2)} + \frac{1}{2}\left(u_{N+(1/2)}\right)^2. \tag{100}$$

The following is similar to what is done at the inlet face, except for the relation between the velocity corrections and the pressure corrections.

We write equation (59) as:

$$u'_{N+(1/2)} = \frac{-1}{A^k_{N,N}}\left[\frac{\partial p'}{\partial x}\right]_{N+(1/2)} \triangle x \approx \frac{-1}{A^k_{N,N}} 2\left(p'_{N+(1/2)} - p'_N\right). \tag{101}$$

Since the outlet pressure is fixed, we put $p'_{N+(1/2)} = 0$, so that:

$$u'_{N+(1/2)} = \frac{-1}{A^k_{N,N}} p'_N. \tag{102}$$

6. Results

We consider two test cases: a one dimensional nozzle flow and a two dimensional flow past a bump in a channel. Both transonic and subsonic conditions are simulated.

6.1 One dimensional nozzle flow

The section of the nozzle varies as:

$$S(x) = \begin{cases} S_{0,} & 0 \le x \le 2L/28 \\ S_0\left\{0.9 + 0.1\left[2\left(\frac{x-(11L/28)}{9L/28}\right)^2 - \left(\frac{x-(11L/28)}{9L/28}\right)^4\right]\right\}, & 2L/28 \le x \le 20L/28 \\ S_{0,} & 20L/28 \le x \le L \end{cases}$$

The non-dimensional length L is 10, and the number of cells is taken 100. The nodes are spaced uniformly.

For compressible flows, it is desirable to have a reasonable guess of the initial pressure and velocity distributions (Demirdžić *et al.*, 1993). We initialize pressure, velocity and temperature based on the following guesses:

$$p_{\text{init}} = p_{\text{out}}, \tag{103}$$

$$M_{\text{init}} = \sqrt{\frac{2}{\gamma - 1}\left[\left(\frac{p_{0,\text{in}}}{p_{\text{out}}}\right)^{(\gamma-1)/\gamma} - 1\right]}, \tag{104}$$

$$T_{\text{init}} = \frac{T_{0,\text{in}}}{1 + ((\gamma - 1)/2))M_{\text{init}}^2}, \tag{105}$$

$$u_{\text{init}} = M_{\text{init}}\sqrt{\gamma T_{\text{init}}}. \tag{106}$$

6.1.1 Transonic flow. We take $p_{0,\text{in}} = 1$ and $T_{0,\text{in}} = 1$. We consider a transonic nozzle with a normal shock at position $15L/28$. Therefore, an outlet pressure $p_{\text{out}} = 0.718025$ has to be imposed.

First, we consider the classical approach, i.e. with Rhie-Chow interpolation and centrally discretized pressure gradient. No underrelaxation was needed and the number of iterations within a time step could be taken as unity. Figure 1(a) shows the Mach number distribution obtained with a first order calculation. Apparently, the shock is extremely smeared out. This fact was also noticed by Moukalled and Darwish (2001). They suggested that a high resolution scheme should be used for both the interface velocities and the interface densities to obtain a sharper shock representation. In our opinion, however, the smearing is not due to the fact that the scheme is only first order accurate. Indeed, Figure 1(b) shows the result with the same pressure-correction procedure, but where the AUSM approach was used. The shock representation is much sharper, even though the upwinding is still only first order accurate.

The extreme smearing of the shock with the classical pressure-correction method, finds its cause in the use of the Rhie-Chow interpolation. As was remarked before, this interpolation introduces a fourth order pressure smoothing term into the momentum equations. This term becomes excessively large when high-pressure gradients occur. In addition, this artificial dissipation, originally introduced in the incompressible case to prevent pressure-velocity decoupling, is not needed anymore when the Mach number is high enough. Thus, one cannot blindly take over the Rhie-Chow interpolation from the incompressible algorithms when designing Mach-uniform methods. However, several examples can be found in the literature where this is done anyway (Demirdžić *et al.*, 1993; Lien *et al.*, 1996; Moukalled and Darwish, 2001).

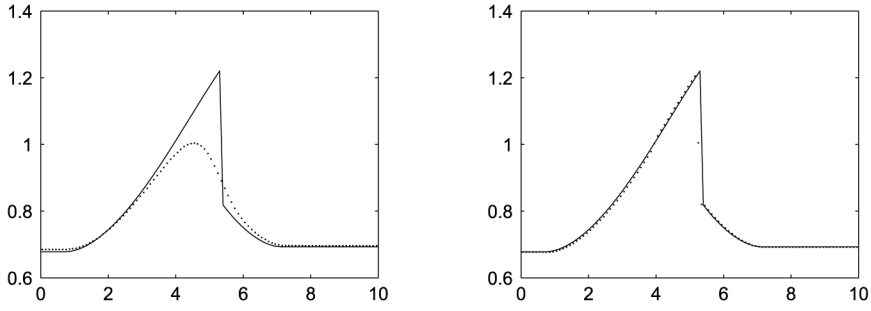

Figure 1.
Mach number distribution for one-dimensional transonic nozzle flow

Notes: Solid line: analytic solution. Symbols: calculation with pressure-correction algorithm, first order upwind. (a) Rhie-Chow interpolation. (b) AUSM+

6.1.2 Subsonic flow. Again $p_{0,\text{in}}$ and $T_{0,\text{in}}$ are equal to one. The outlet pressure p_{out} is taken 0.9944. Doing so, a throat Mach number of 0.09967 is obtained. Underrelaxation was needed to be able to converge and several iterations per time step had to be taken. The fact that underrelaxation is needed in low Mach number flow was also noticed by other authors (Batten *et al.*, 1996; Issa and Javareshhkian, 1998; Moukalled and Darwish, 2001).

For low Mach number flow, the classical approach can be used. The AUSM approach can be used as well, if the afore-mentioned adaptations with regard to scaling and pressure-velocity coupling are done. Figure 2(a) shows the Mach number distribution obtained with a first order calculation.

If the preconditioning in the convective fluxes is switched off, the algorithm becomes unstable. This is also the case when the pressure diffusion term (42) is removed. After a small number of time steps, when steady state is not yet reached, the creation of oscillations can be seen (Figure 2(b)).

Edwards and Liou (1998) remark themselves that the form (42) of the interface mass flux shares a close relationship with the momentum interpolation procedure developed by Rhie and Chow. This was also noticed by Venkateswaran and Merkle (1997). However, the essential difference with the Rhie-Chow interpolation is that the pressure-diffusion term added to the AUSM flux is turned off as the sonic speed is reached. As a result, it cannot cause excessive smearing of shocks as was the case with the Rhie-Chow interpolation.

6.2 Flow past a bump in a channel

As a second test case, the two dimensional inviscid flow past a bump in a channel is taken. Different inlet Mach numbers M_{in} are considered, so that flows ranging from low Mach subsonic to transonic are obtained. Two different grids are used, a coarse one and a finer one. Both are stretched. The coarse grid has 48×16 cells, the finer grid has 96×32 cells. They are shown in Figure 3.

6.2.1 Transonic flow. An inlet Mach number $M_{\text{in}} = 0.85$ gives a transonic flow with a normal shock. Figure 4 shows the Mach contours obtained with both the classical Rhie-Chow interpolation and the AUSM+ scheme, for a second order calculation on the coarse grid (16×48 cells). Clearly, a much sharper shock representation is obtained when the AUSM+ flux is used.

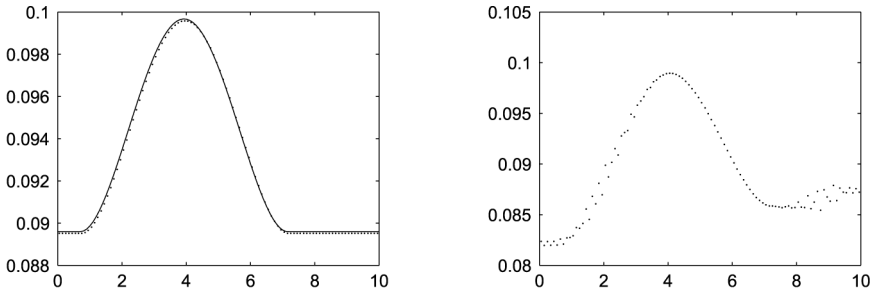

Notes: Solid line: analytic solution. Symbols: calculation with pressure-correction algorithm. (a) AUSM+, with low Mach adaptations, steady state. (b) AUSM+, without pressured diffusion term, intermediate state

Figure 2.
Mach number distribution for one-dimensional subsonic nozzle flow

The latter can also be observed from the Figure 5 where the Mach number profiles along the upper and lower well are shown. Figure 5(a) shows the results for a first order calculation. The coarse grid results (16 × 48 cells) again show the sharper shock representation for the AUSM+ scheme than for the Rhie-Chow interpolation. If the finer grid (32 × 96 cells) is used, also the Rhie-Chow interpolation gives a sharper shock representation. This was also observed in (Demirdžić *et al.*, 1993) and is obvious, as the dissipation diminishes for smaller grid sizes. Notice that even for the fine grid calculation, the Rhie-Chow interpolation still gives more smearing than the AUSM+ calculation on the coarse grid. The same conclusion holds for a second order calculation (Figure 5(b)). Obviously, the schock representation is sharper than for the first order calculation. This is the case for all the schemes.

6.2.2 Subsonic flow. As a low subsonic flow example, the case of an inlet Mach number $M_{\text{in}} = 10^{-5}$ is considered. Again, the calculation can be done with the classical approach or with the AUSM approach including low Mach adaptations. The Mach number profiles along the walls are shown in Figure 6. The coarse grid (48 × 16 cells) was used and k was taken 1/3 (equation (13) and (14)). The results are quasi identical for each of the methods.

7. Conclusion

We have presented a Mach uniform pressure-correction algorithm, and illustrated its performance with two test cases for transonic and subsonic flow. In the transonic case, the classical Rhie-Chow interpolation causes excessive smearing of the shock. With the use of AUSM+ fluxes, a much sharper shock representation is obtained. For the subsonic case, special measures have to be taken to keep the fluxes properly scaled and to prevent pressure-velocity decoupling. In this way, we achieved extension of a popular numerical algorithm from a density-based and coupled, to a pressure-based and segregated formulation.

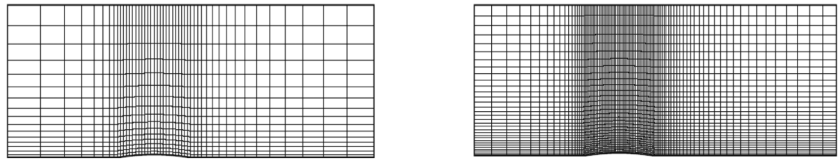

Notes: Left: coarse grid, 48x16 cells. Right: fine grid, 96x32 cells

Figure 3.
Grids used for the flow past a bump in a channel

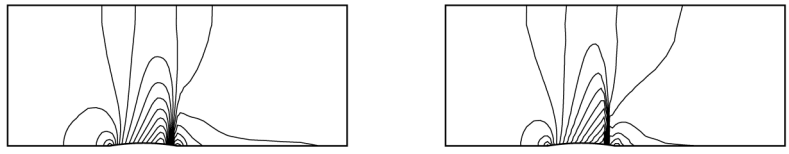

Notes: Second order calculation. Grid 48x16. Left: Rhie-Chow interpolation. Right: AUSM+ flux

Figure 4.
Mach number contours, $M_{\text{in}} = 0.85$

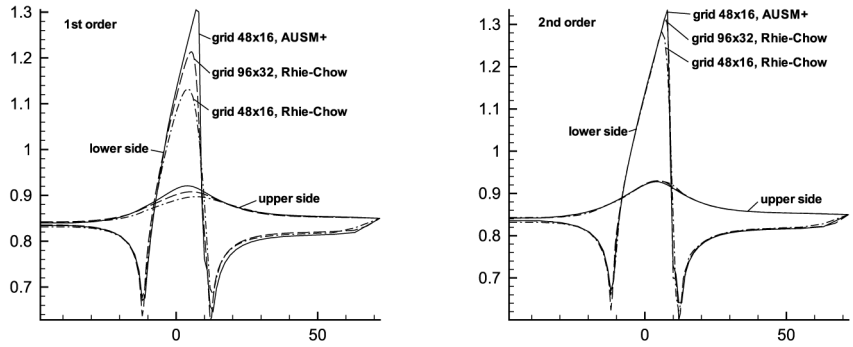

Notes: Second order calculation. Solid line: grid 48x16, AUSM+ flux. Dashed line: grid 96x32, Rhie-Chow interpolation. Dash-dotted line: grid 48x16, Rhie-Chow interpolation. (a) First order calculation. (b) Second order calculation

Figure 5.
Mach number profiles along the upper and lower wall, $M_{in} = 0.85$

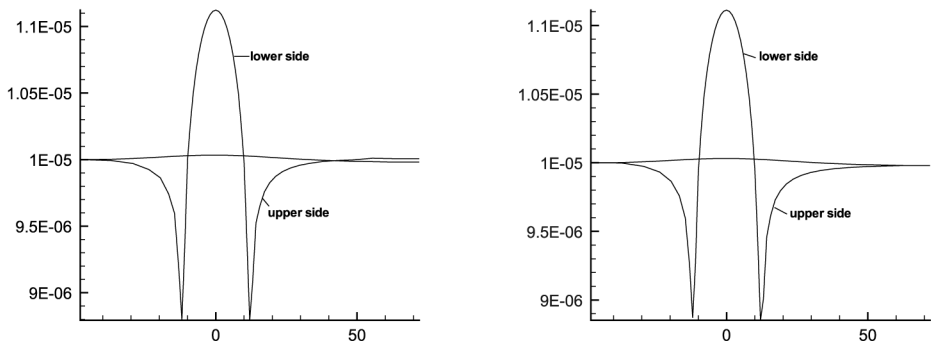

Notes: Left: Rhie-Chow interpolation. Right: AUSM+ flux with low Mach adaptations

Figure 6.
Mach number profiles along the upper and lower wall, $M_{in} = 10^{-5}$

References

Batten, P., Lien, F.S. and Leschziner, M.A. (1996), "A positivity-preserving pressure-correction method", *Proceedings of the 15th International Conference on Numerical Methods in Fluid Dynamics*, Vol. 490 of Lecture Notes in Physics, Springer, pp. 148-51.

Bijl, H. and Wesselling, P. (1998), "A unified method for computing incompressible and compressible flows in boundary-fitted coordinates", *Journal of Computational Physics*, Vol. 141, pp. 153-73.

Davidson, L. (1996), "A pressure-correction method for unstructured meshes with arbitrary control volumes", *International Journal for Numerical Methods in Fluids*, Vol. 22, pp. 265-81.

Demirdžić, I., Lilek, Ž. and Perić, M. (1993), "A collocated finite volume method for predicting flows all speeds", *International Journal for Numerical Methods in Fluids*, Vol. 16, pp. 1029-50.

Edwards, J.R. and Liou, M-S. (1998), "Low-diffusion flux-splitting methods for flows at all speeds", *AIAA Journal*, Vol. 36, pp. 1610-7.

Edwards, J.R., Franklin, R.K. and Liou, M-S. (2000), "Low-diffusion flux-splitting methods for real fluid flows with phase transitions", *AIAA Journal*, Vol. 38 No. 9, pp. 1624-33.

Hirsch, C. (1990), *Numerical Computation of Internal and External Flows*,Vol. 2, Wiley, New York, NY.

Issa, R.I. and Javareshhkian, M.H. (1998), "Pressure-based compressible calculation method utilizing total variation diminishing schemes", *AIAA Journal*, Vol. 36 No. 9, pp. 1652-7.

Lien, F.S. and Leschziner, M.A. (1994), "Upstream monotonic interpolation for scalar transparent with application to complex turbulent flows", *International Journal for Numerical Methods in Fluids*, Vol. 19, pp. 527-48.

Lien, F.S., Chen, W.L. and Leschziner, M.A. (1996), "A multiblock implementation of a non-orthogonal, collocated finite volume algorithm for complex turbulent flows", *International Journal for Numerical Methods in Fluids*, Vol. 23, pp. 567-88.

Liou, M-S. (1996), "A sequel to AUSM; AUSM + ", *Journal of Computational Physics*, Vol. 129, p. 364.

Liou, M-S. (2000), "Mass flux schemes and connection to shock instability", *Journal of Computational Physics*, Vol. 160, pp. 623-48.

Liou, M-S. and Steffen, C.J. (1993), "A new flux splitting scheme", *Journal of Computational Physics*, Vol. 107, pp. 23-39.

Luo, H. and Baum, J.D. (2003), "Extension of HLLC scheme for flows at all speeds", AIAA Paper, 03-3840.

Merkle, C.L., Venkateswaran, S. and Buelow, P.E.O. (1992), "The relationship between pressure-based and density-based algorithms", AIAA Paper, 92-0425.

Moukalled, F. and Darwish, M. (2001), "A high-resolution pressure-based algorithm for fluid flow at all speeds", *Journal of Computational Physics*, Vol. 168, pp. 101-33.

Patankar, S.V. (1980), *Numerical Heat Transfer and Fluid Flow*, Hemisphere, New York, NY.

Patankar, S.V. and Spalding, D.B. (1972), "A calculation procedure for heat, mass and momentum transfer in three-dimensional parabolic flows", *International Journal of Heat and Mass Transfer*, Vol. 15, pp. 1787-806.

Perić, M., Kessler, R. and Scheuerer, G. (1988), "Comparison of finite-volume numerical methods with staggered and colocated grids", *Computers & Fluids*, Vol. 16 No. 4, pp. 389-403.

Rhie, C.M. and Chow, W.L. (1982), "Numerical study of the turbulent flow past an isolated airfoil with trailing edge separation", *AIAA Journal*, Vol. 21 No. 11, pp. 1525-32.

Senocak, I. and Shyy, W. (2002), "A pressure-based method for turbulent cavitating flow computations", *Journal of Computational Physics*, Vol. 176, pp. 363-83.

Shyy, W., Thakur, S.S., Ouyang, H., Liu, J. and Blosch, E. (1997), *Computational Techniques for Complex Transport Phenomena*, Cambridge University Press, Cambridge.

Van der Heul, D.R., Vuik, C. and Wesseling, P. (2003), "A conservative pressure correction method for flow at all speeds", *Computers & Fluids*, Vol. 32, pp. 1113-32.

Venkateswaran, S. and Merkle, C.L. (1997), "Evaluation of artificial dissipation models and their relationship to the accuracy of Euler and Navier-Stokes computations", *Proceedings of 16th International Conference on Numerical Methods in Fluid Dynamics*.

Vierendeels, J., Merci, B. and Dick, E. (2001), "Blended AUSM+ method for all speeds and all grid aspect ratios", *AIAA Journal*, Vol. 39 No. 12, pp. 2278-82.

Weiss, J.M. and Smith, W.A. (1995), "Preconditioning applied to variable and constant density flows", *AIAA Journal*, Vol. 33 No. 11, pp. 2050-7.

Wenneker, I., Segal, A. and Wesseling, P. (2002), "A Mach-uniform unstructured staggered grid method", *International Journal for Numerical Methods in Fluids*, Vol. 40, pp. 1209-35.

About the authors

Krista Nerinckx was born on November 1, 1979 in Gent, Belgium; MSc in Electromechanical Engineering, Ghent University 2002. PhD student at Ghent University since October 2002, supported by the Flemish Institute for the Promotion of Scientific and Technological Research in the Industry (IWT). Teaching: exercises turbomachinery. Area of research: computational fluid dynamics, Mach-uniform algorithms, pressure-correction methods. Publications: about five papers in international scientific conferences. Krista Nerinckx is the corresponding author and can be contacted at: Krista.Nerinckx@Ugent.be

Jan Vierendeels was born on November 27, 1973 in Dendermonde, Belgium; MSc in Electromechanical Engineering, Ghent University 1991; MSc in Aeronautics and Astronautics, Ghent University 1993; MSc in Biomedical Engineering, Ghent University 1996; PhD in Computational Fluid Dynamics, Ghent University 1998. Researcher and Senior Researcher at Ghent University from June 1992 to September 2002; Associate Professor at Ghent University since October 2002. Teaching: transport phenomena, fluid mechanics, aeroplanes. Area of research: CFD algorithms, fluid-structure interaction, complex flows. Publications: about 35 articles in international scientific journals and about 90 papers in international scientific conferences.

Erik Dick was born on December 10, 1950 in Torhout, Belgium; MSc in Electromechanical Engineering, Ghent University 1973; PhD in Computational Fluid Dynamics, Ghent University 1980. Researcher, Senior Researcher, Head of Research and Lecturer at Ghent University from August 1973 to June 1991; Associate Professor at University of Liège from July 1991 to September 1992; Associate Professor at Ghent University from October 1992 to September 1995; Full Professor since October 1995; Head of the Department of Flow, Heat and Combustion Mechanics since October 1997. Teaching: turbomachinery, gas turbines, computational fluid dynamics. Area of research: computational fluid dynamics, engineering models for turbulence and transition. Publications: about 80 articles in international scientific journals and about 180 papers in international scientific conferences.

To purchase reprints of this article please e-mail: **reprints@emeraldinsight.com**
Or visit our web site for further details: **www.emeraldinsight.com/reprints**